July 27, 2023

Jacob Eapen
Dina Elgewaily

K. L. Murty (NCSU), Rick Ubic (BSU), Karthik Chinnathambi (BSU), Anne Campbell (ORNL)
Abbie Jones (UoM), Alex Theodosiou (UoM), Graham Hall (UoM), Barry J. Marsden (UoM)

Quantifying the Dynamic and Static Porosity/Microstructure Characteristics of Irradiated Graphite through Multi-technique Experiments and Mesoscale Modeling

NC STATE UNIVERSITY

DOE ART Gas-Cooled Reactor (GCR) Review Meeting
July 25 – 27, 2023

ART Advanced Reactor Technologies

Pores in Nuclear Graphite Grades

- All graphite grades are porous; porosity varies between 14 to 22%.
- Pores are formed during manufacturing process as well as in in-service (reactor) conditions.
- It's typical to report only a macroscopic measure of porosity, which is defined as the pore volume to the total volume.

Grade	Grain Type	Grain Size (μm)	Density (g/cm^3)	Porosity (%)
NBG-18	Large	1600	1.85	14
NBG-17	Medium	800	1.89	14
PCEA	Medium	800	1.84	16
IG-110	Fine	20	1.77	21
G347A	Superfine	11	1.85	-
AXF/ZXF 5Q	Ultrafine	1–5	1.78	20

Importance of Pore Metrics

- Pore size, shape, and connectivity determine the transport of fission products or ingress of external agents (molten salt, air, water etc).
- Unit diffusivity of many species in graphite is known. The pore pathways have a compounding effect of diffusion and transport.
- Pore connectivity is instrumental in pore-pore interactions. With irradiation, small pores coalesce and become bigger ones.
- A knowledge of a realistic pore structure is needed for physics-based modeling (such as phase-field).

Pores Size Distribution and Methods

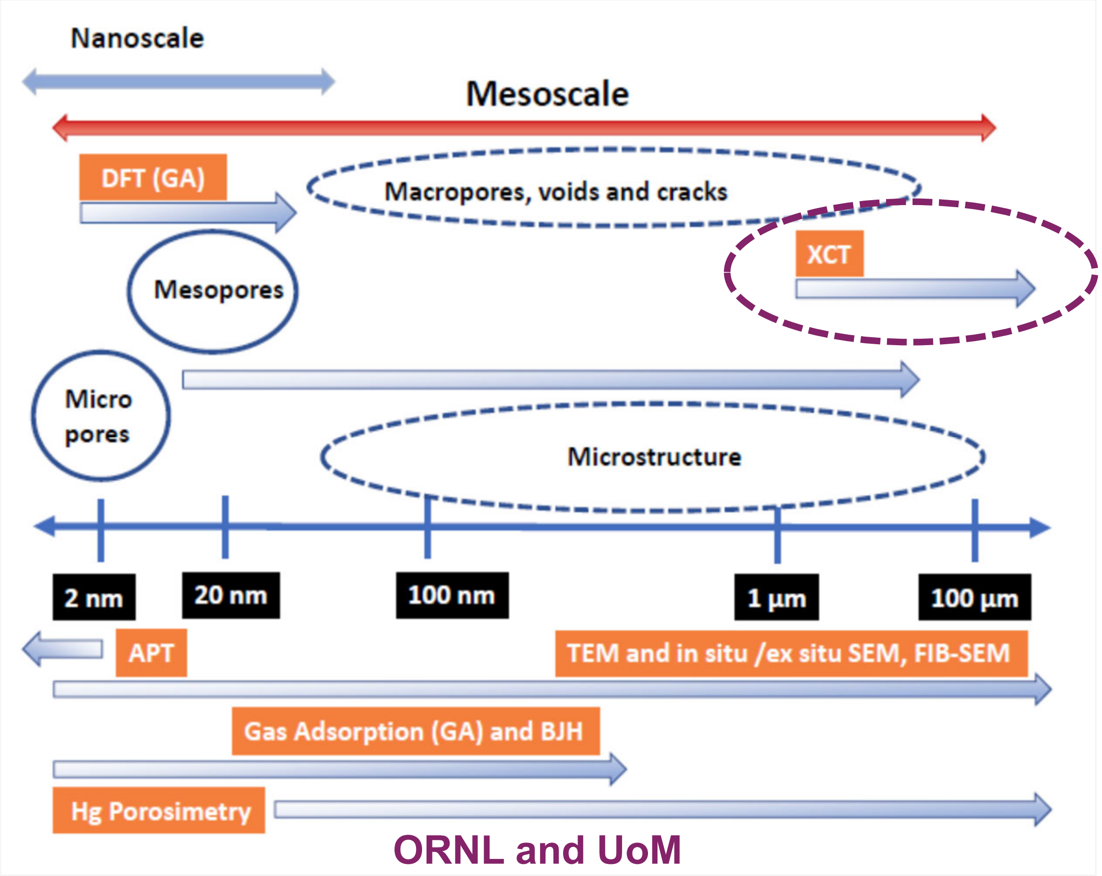

NC State

BSU

ORNL and UoM

Xray Computed Tomography (XCT)

- **ZEISS Xradia 510 Versa X-ray microscopes (XRM)**
- High-resolution 3D X-ray imaging system.
- Allows submicron imaging of samples from mm to inches with weight up to 15 kg and sample size up to 300 mm.
- Achieves < 0.7 µm true spatial resolution.
- Xray source: 30-160kV, 10W maximum power.

Intensity is limited for low Z materials such as graphite.

XCT Analysis:
Controlled Samples with Known Porosity

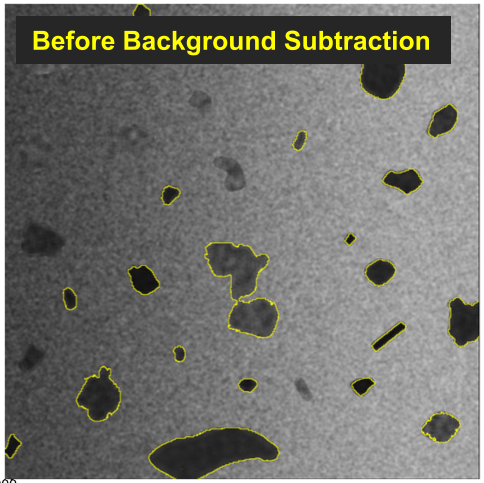

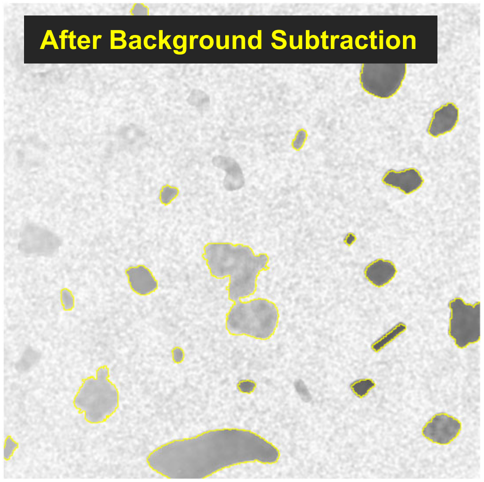

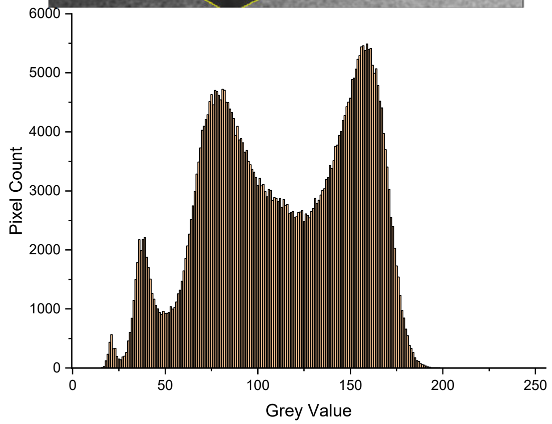

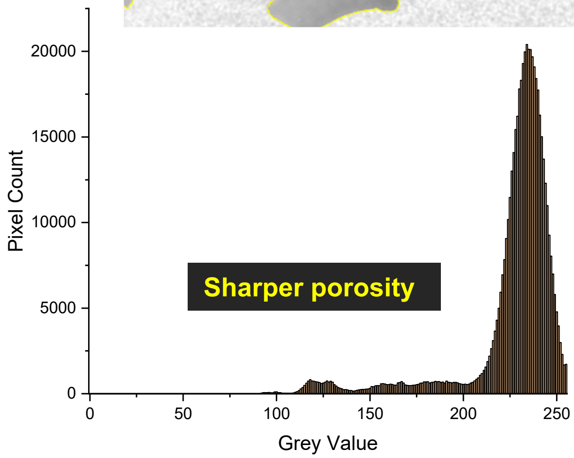

Analysis with Different Methods

- Huang
- Intermodes
- **IsoData**
- IJ_IsoData
- Li
- Max Entropy
- Mean
- Minimum
- Moments
- **Otsu**
- Percentile
  Renyi Entropy
- Shanbhag
- Traingle
- Yen

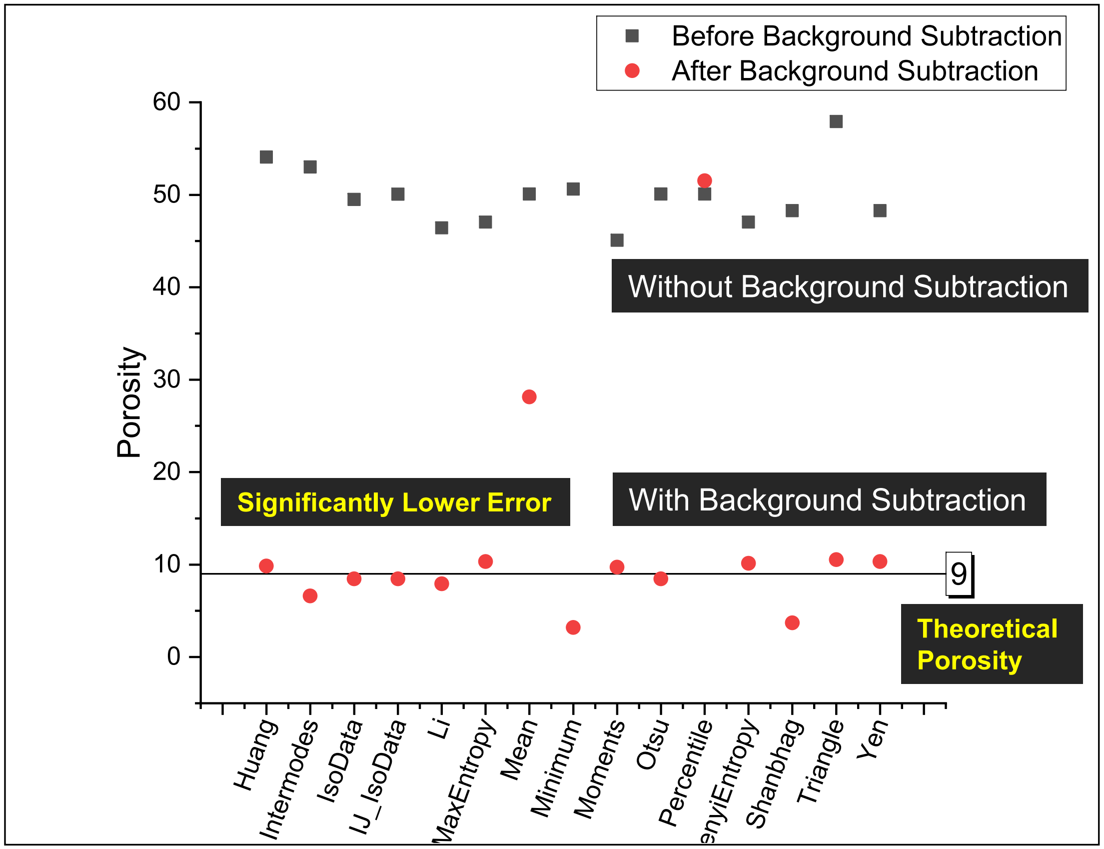

Most methods worked; Isodata and Otsu algorithms performed the best!

Case Study: Ag deposited AXF-5Q Grade

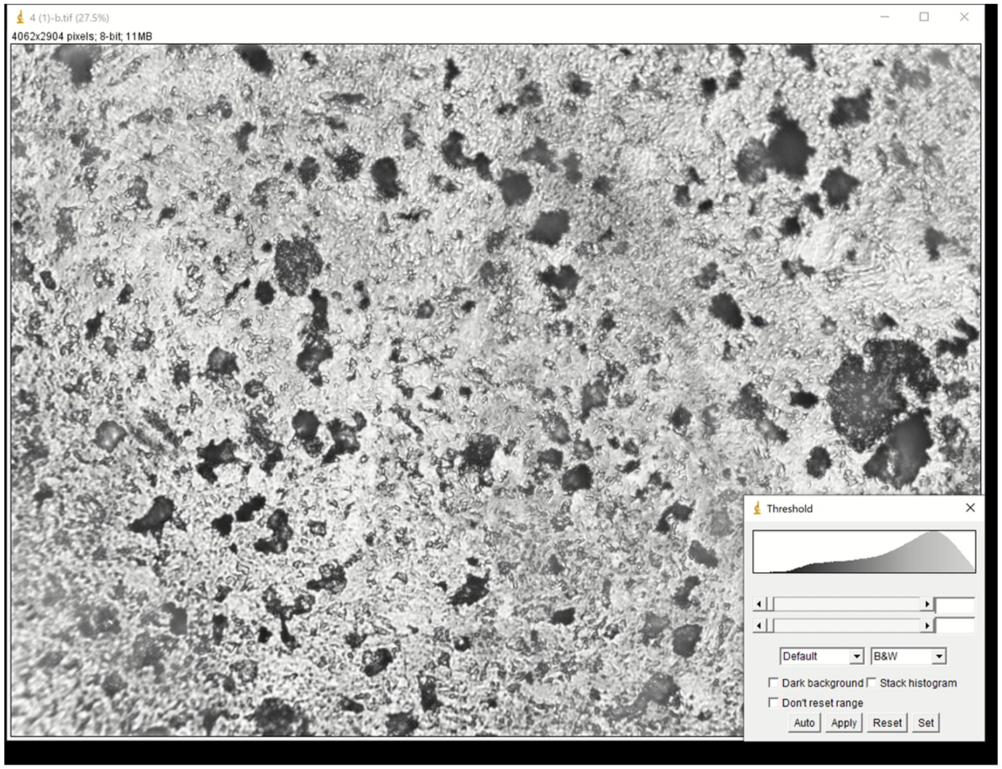

Performance of Different Algorithms

- Huang
- Intermodes
- **IsoData**
- IJ_IsoData
- Li
- Max Entropy
- Mean
- Minimum
- Moments
- **Otsu**
- Percentile
  Renyi Entropy
- Shanbhag
- Traingle
- Yen

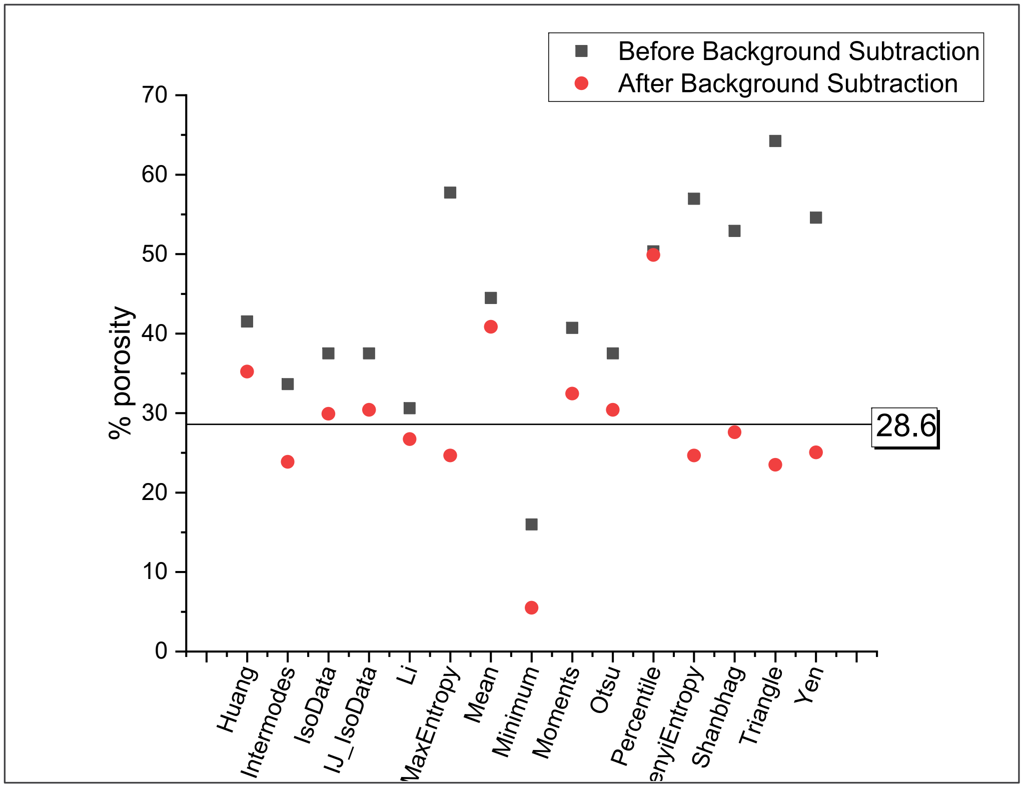

Wide scatter!

Need a better approach.

AXF–5Q 3D XCT Analysis

- Three different cubic samples of size ~5 mm^3 are scanned at 20x magnification, using fixed parameters.
- Post reconstruction, the resulting tiff images are cropped down to 330 x 340 pixels to exclude air around the sample as well as edge effects.

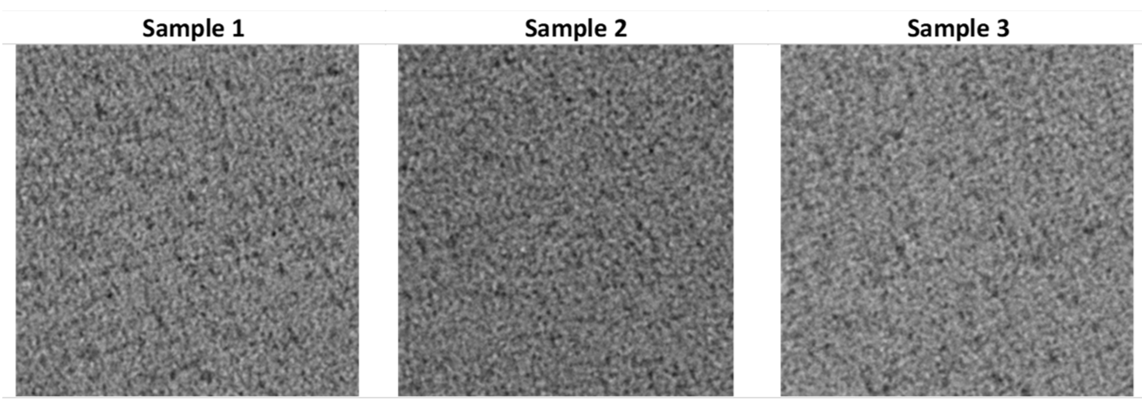

Representative slices from each sample.

Magnification	20x
Current (mA)	90
Voltage (kV)	100
Exposure time (s)	10
Image Height (pixel)	492
Image Width (pixel)	441
Images taken (slices)	478
Pixel size (microns)	0.95
Detector to sample distance (mm)	52.4
Source to sample distance (mm)	29.1

CT scan parameters used for the three samples.

Thresholding Problem

- Low Z value of carbon limits the contrast between solid graphite and the grey value of air in the pores.
- The resulting histogram is, therefore, not bimodal enough to allows reasonable thresholding using global thresholding.
- Only one peak is discernible, causing both Otsu and IsoData methods to cut off the porosity at over 40%, which can be refuted by visual inspection in comparison to the original image.

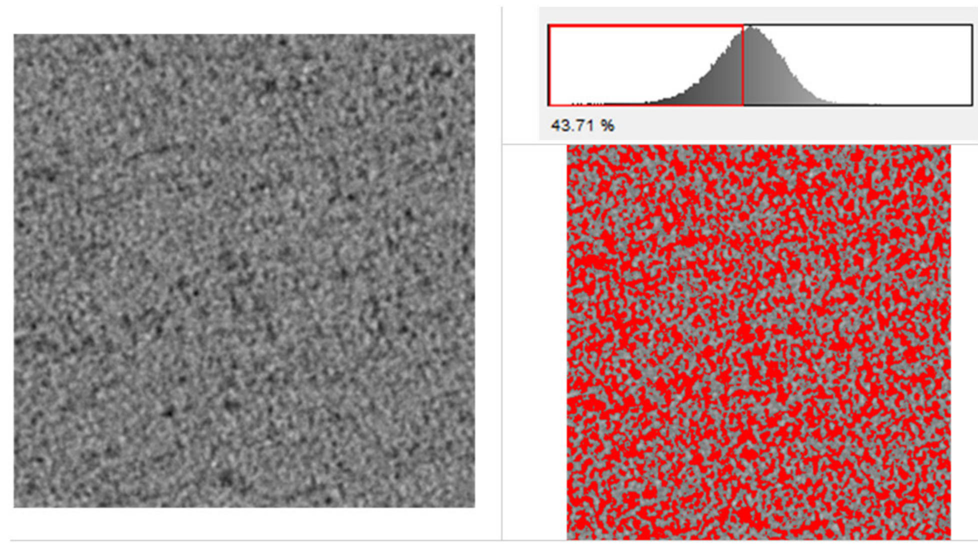

Example slice and its thresholded pore space using Otsu method.
Porosity = 43.71%

Machine Learning Approach

- A training data set is used to differentiate pores and matrix regions.
- Two classes are created to represent the pores and the background. A few sure pores and parts of the background are then outlined in several slices to specify which voxels the user wants to consider as black (pores) or white (graphite).
- The FastRandomForest classifier is trained on the input voxels to assign new gray values to voxels based on their local gradient with respect to the nearest outlined voxels, using one of several filter options.

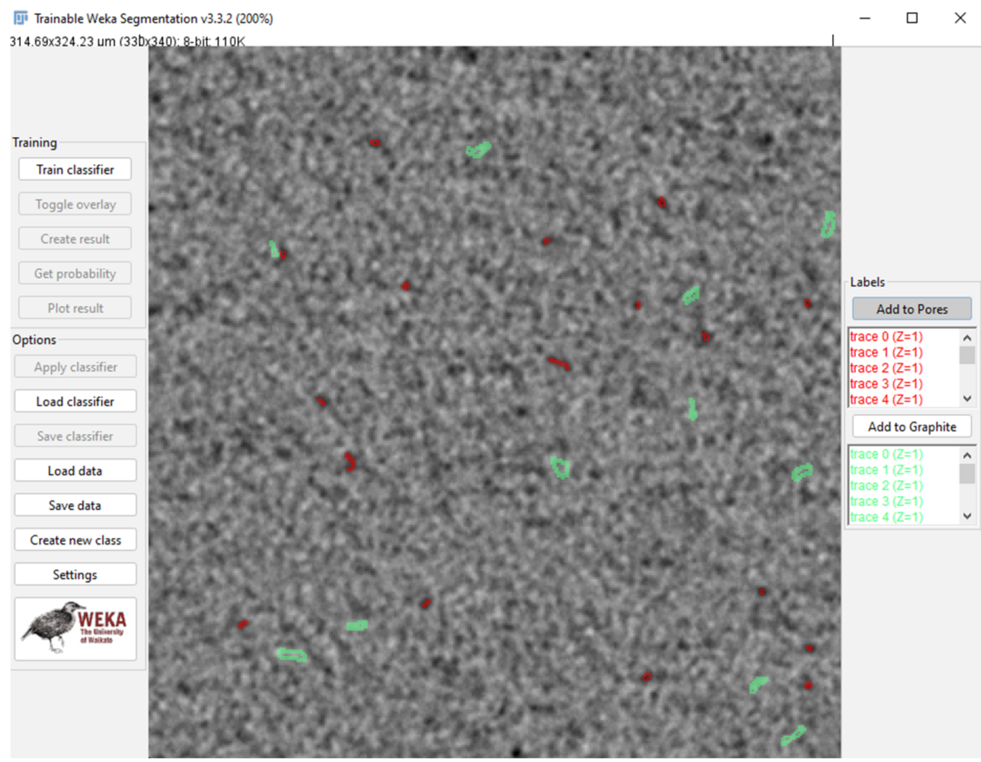

Training data for one slice

Collaboration with A. Rabbani, University of Leeds

Machine Learning Approach

- The resulting segmentation is then inspected visually, to check for proper inclusion of all training inputs.
- The training process is repeated until the out-of-bag error converges below 3%
- Out-of-bag (OOB) error is the average error in predicting the results of each tree from all the trees that did not contain that tree during training.

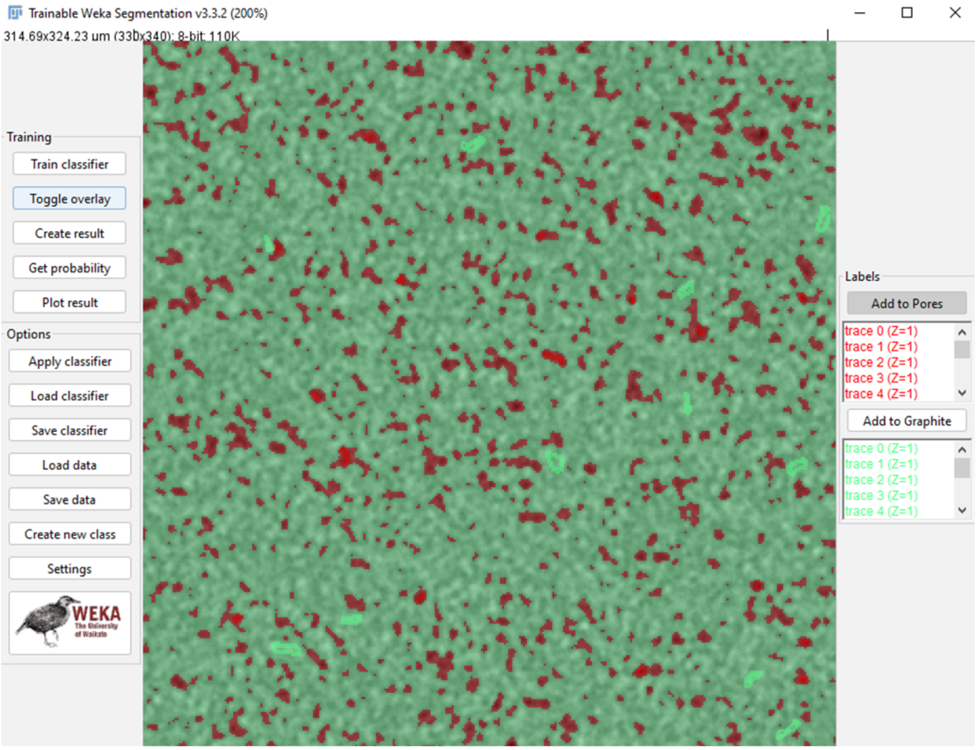

Example training results for one slice

Machine Learning Approach: Bimodal Distribution

- Probability maps are created to show the confidence with which voxels are claimed under pores or graphite, represented in their gray values.

- The resulting image histogram is now **bimodal** enough to produce very similar results for porosity (17-20%) when segmented using most thresholding techniques.

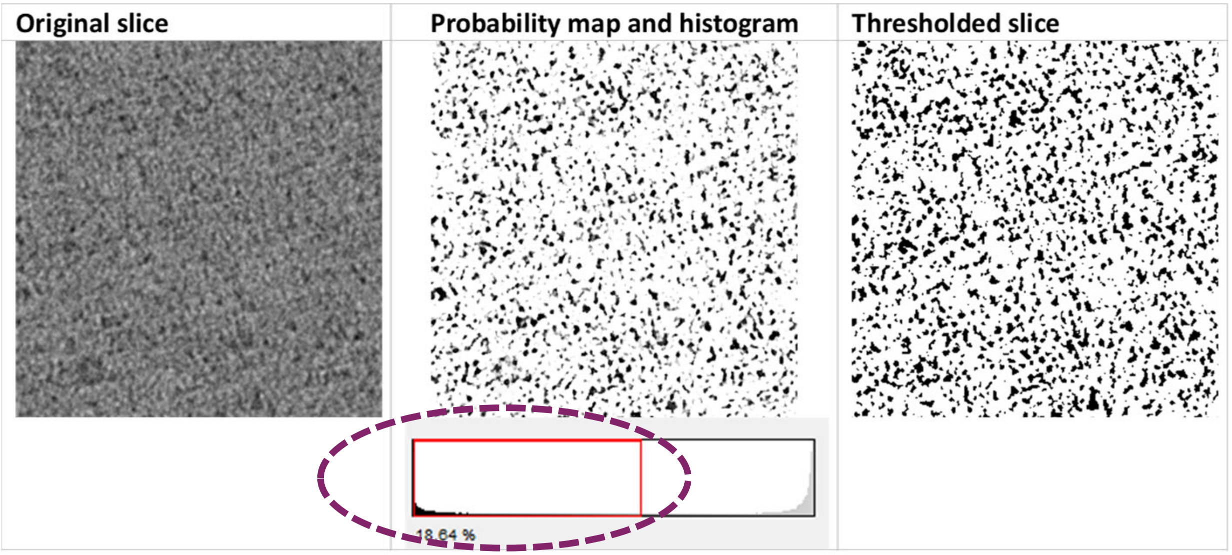

Example slice with its resulting probability map, histogram, and Otsu thresholding

Representative Element Volume (REV) Analysis

- What is the smallest representative volume statistically?
- Relative gradient error of porosity – in all directions – is calculated in increasingly large element volumes.
- Porosity is calculated for each volume, and the REV is reached when the relative gradient error of porosity reaches below 0.2.

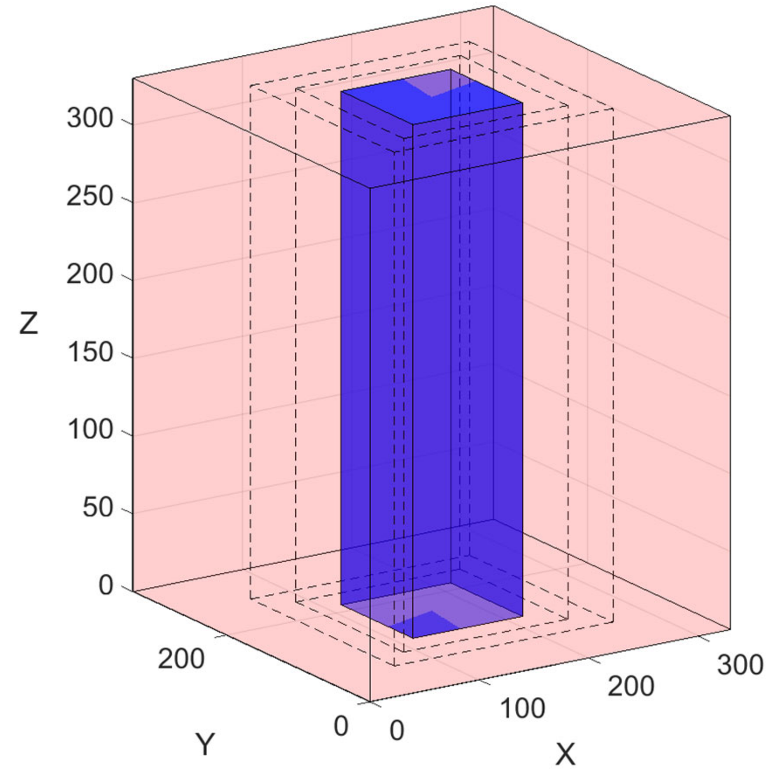

Schematic of the REV within the original volume with increasing width but same height.

Collaboration with A. Rabbani, Leeds

Representative Element Volume (REV) Analysis

- For the three samples, porosity seems to converge around ~17-18%.
- The relative gradient error, averaging over all directions, falls below 0.2 around 100 microns (105 voxels) which is ~30% of the original volume.

Sample 1 | Sample 2 | Sample 3

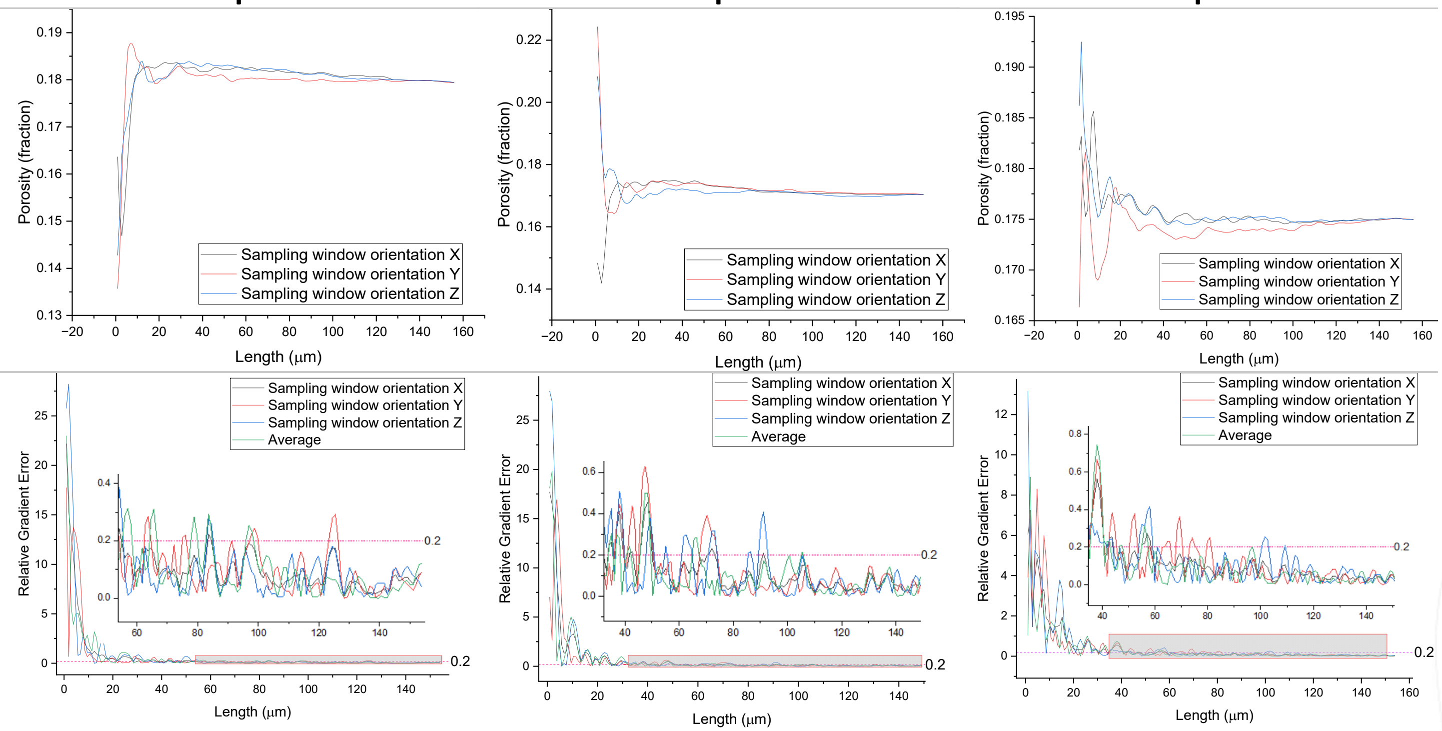

REV analysis of the three samples. (Top) is calculated porosity in 3 directions. (Bottom) is calculated relative gradient error

Pore Segmentation

- The Euclidean distance transform of the inverse REVs are calculated to represent the distances between centers of neighboring pores.
- A gaussian blur filter is applied to the Euclidean distance map to avoid over segmentation.

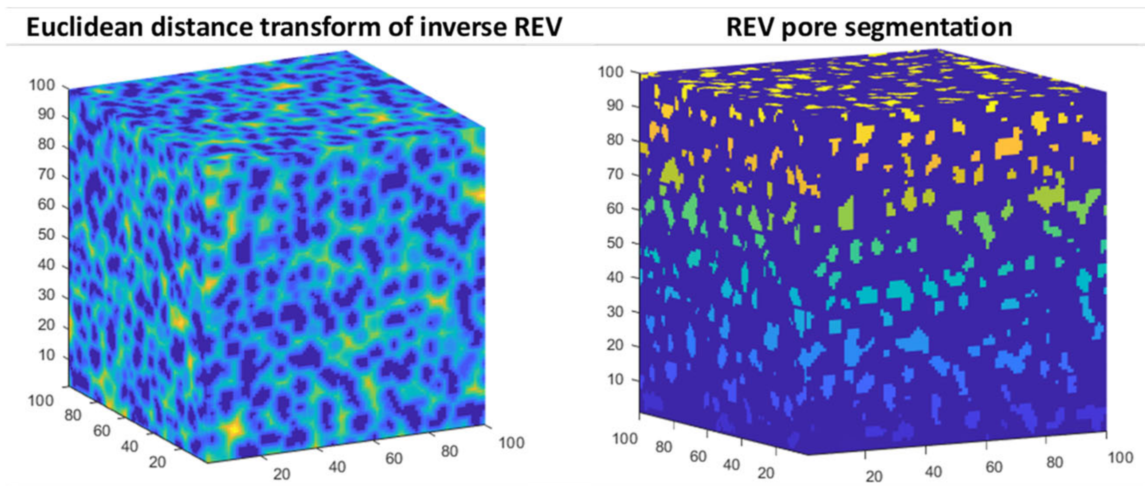

Euclidean distance transform of inverse REV (left), and the resulting REV pore segmentation (right)

Pore Size: Equivalent Radius

- The equivalent radius of each pore is calculated by: $R_{eqv} = Res \times \left(\frac{3\times\text{volume}}{4\pi}\right)^{\frac{1}{3}}$ where Res is the scan resolution, and volume is the number of voxels per pore.
- Average pore size for the 3 samples seems to be ~2.3 microns with similar normal distributions ranging from 0.5 to 5.5 microns.
- The reported pore size in the AXF-5Q manufacturers sheet is 0.8 microns.

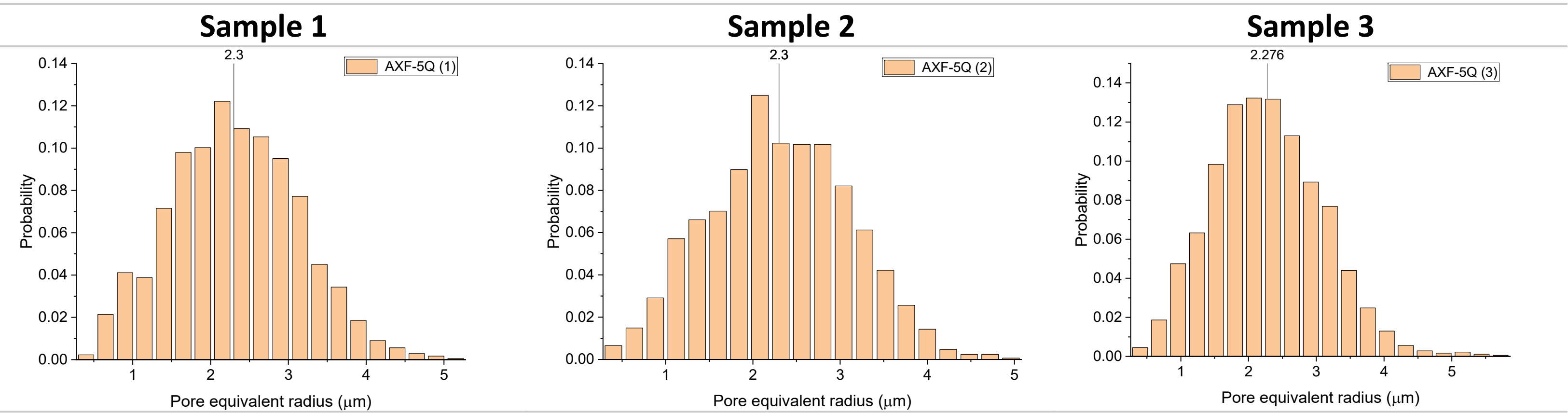

Pore size distributions of the three REVs

Solidity: Deviation from Sphericity

- Solidity is defined by the ratio of the shape's true volume (number of voxels within edges) to its convex volume, with convex volume being that of the polygon connecting all the corners of that shape. It therefore takes values from 0 to 1. **The higher the solidity, the closer the shape is to a perfect sphere**.
- Smaller pores are likelier to be more spherical and vice versa.

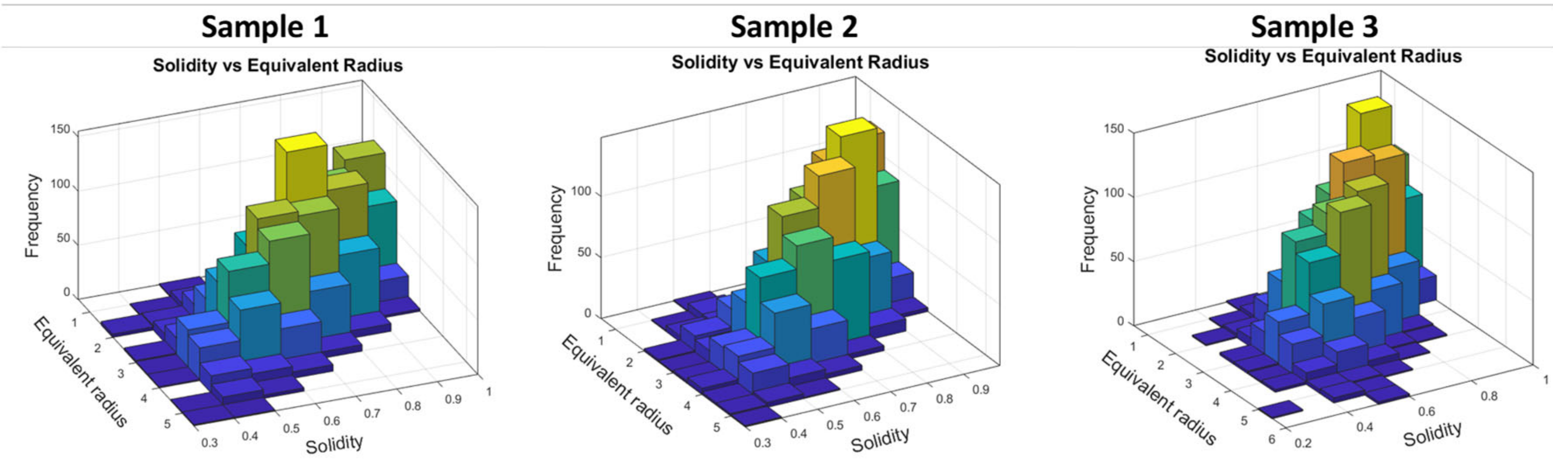

Solidity distribution with respect to pore equivalent radii for the three REVs

Pore Connectivity

- Centroids (positions of pore centers) are calculated based on their shape and volume. Spherical nodes are drawn at the centroids, and their colors are mapped to the pores equivalent radii.
- The number of connections is represented by straight lines (edges) between each pore center and its touching neighbors, with their colors mapped to the lengths of connections

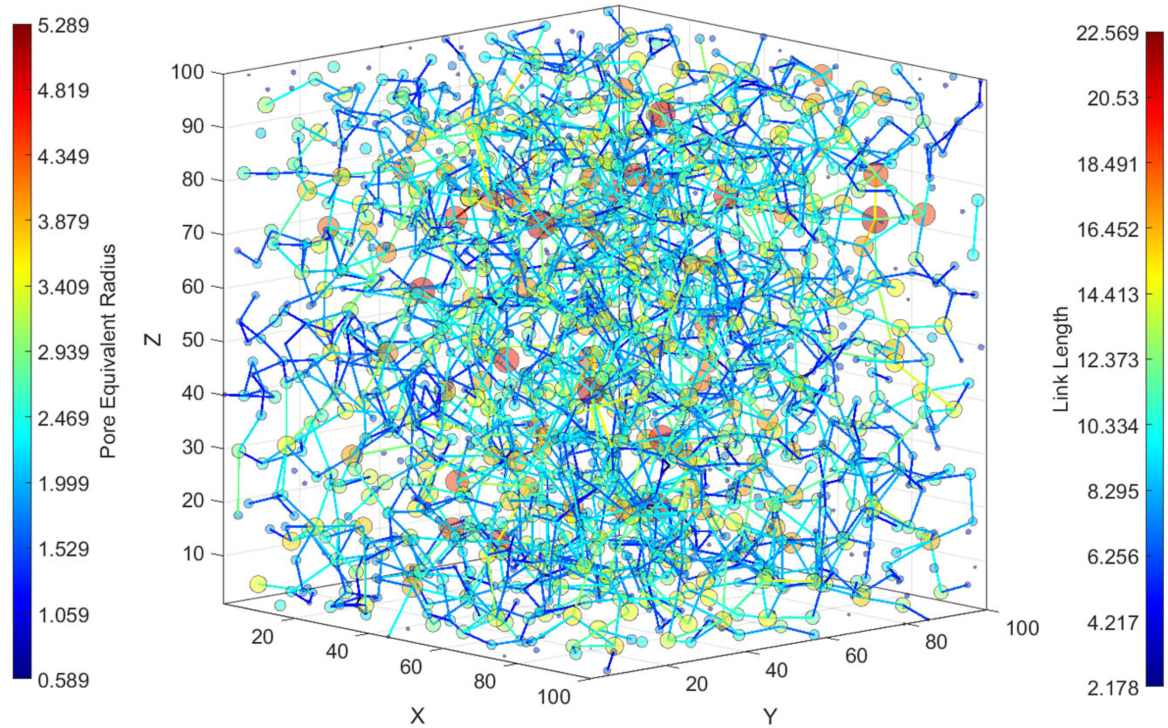

Pore connectivity network. Pores are color-coded by size, and links are color-coded by length.

Pore Coordination Number

- Similar distributions of the number of connections per pore (coordination number) for the three samples, with the average coordination number being ~2.6 in each sample.

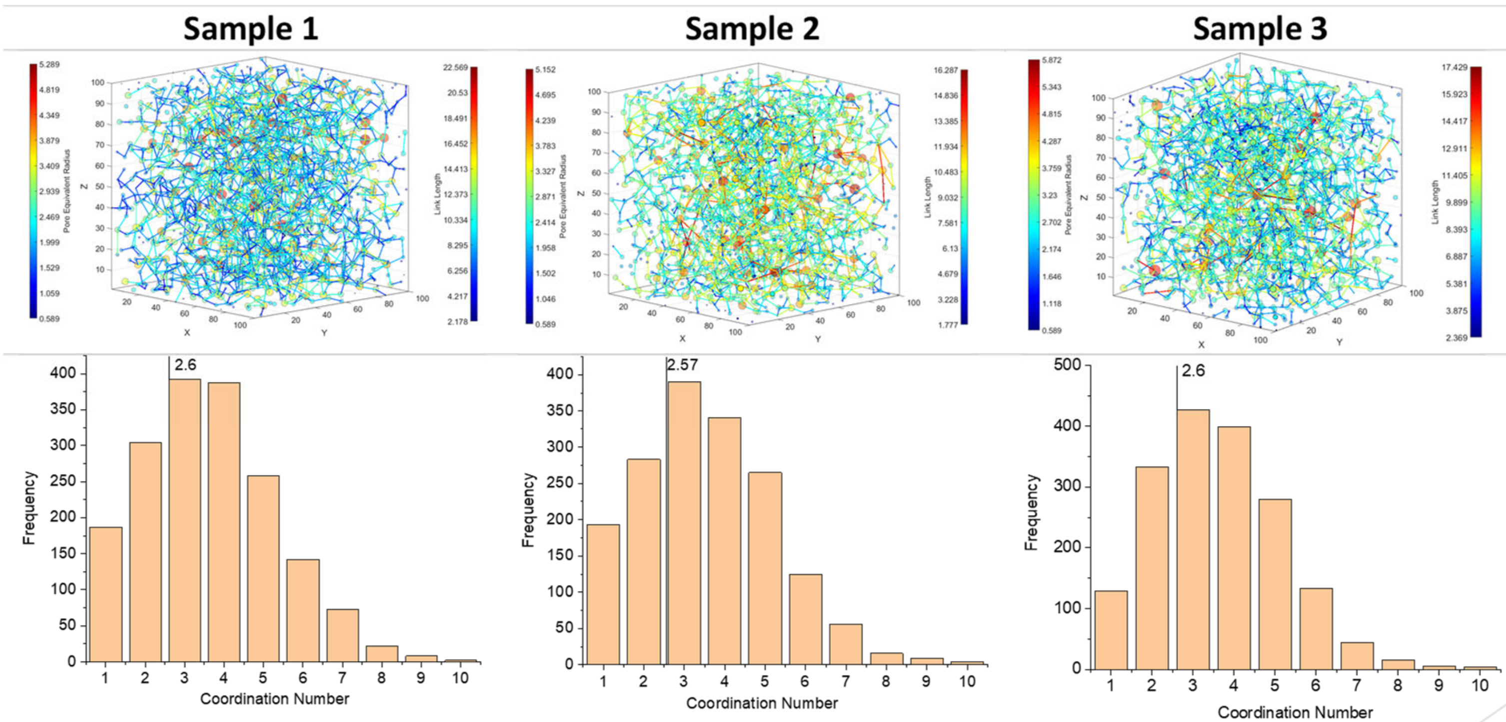

Pore connectivity network of the three REVs, and their corresponding pore coordination number distribution.

Pore Connectivity Matrix

- A connectivity matrix representing the extracted pore network is found by detecting and recording adjacent pore spaces with unique labels over 3-D 18-connected neighborhoods.
- The matrix is symmetrical around x=y as each connection is counted twice. Most connections seem to be between average sized pores with little to no connections occurring between larger pores. The bottom panel shows the density map of each matrix.

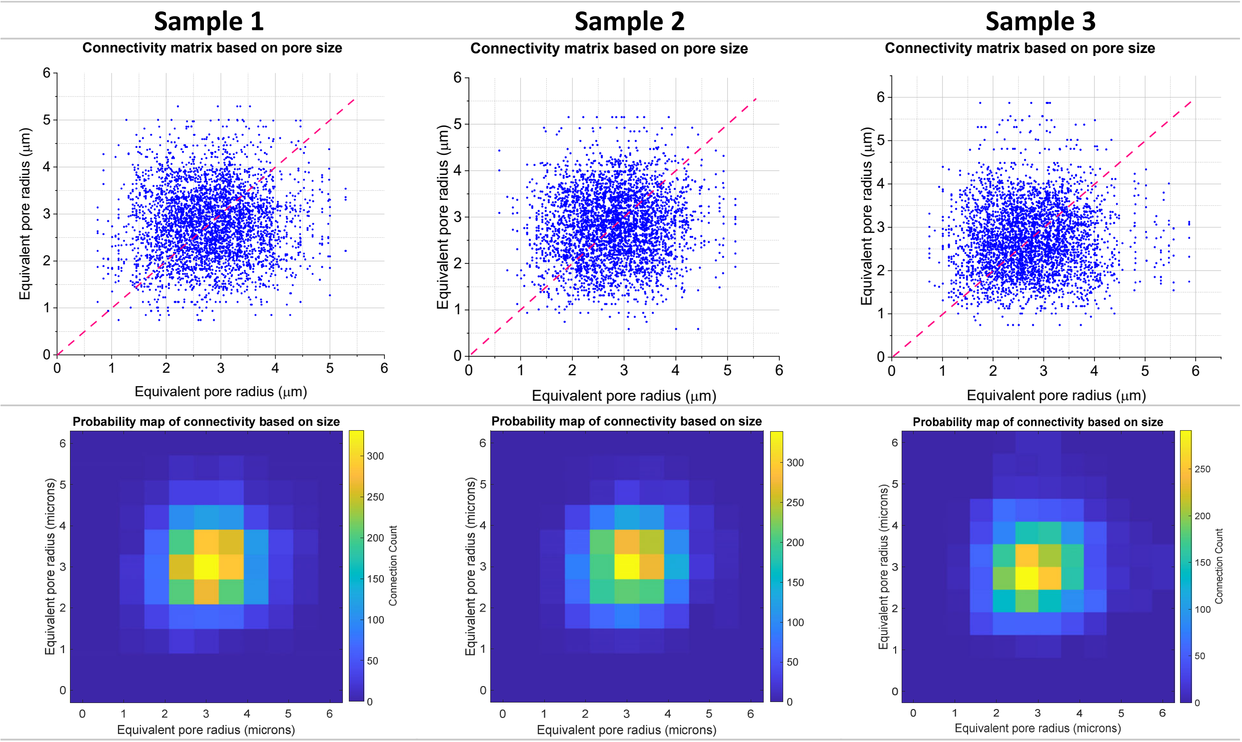

Pore connectivity matrix by pore size (top) and density maps of said matrix (bottom)

Open and Closed Porosity

- Open pores are those connected to the outer surface in any direction. To divide the pore space into open and closed pores, a layer of empty voxels is added to the entire REV surface before re-segmenting the pore space, and then removed, so that the segmented volume represents the two classes (open and closed pores).
- Between the three samples, closed porosity seem to be ~4-7%
- The reported closed porosity in the AXF-5Q manufacturers sheet is ~20%.

Sample 1	Sample 2	Sample 3

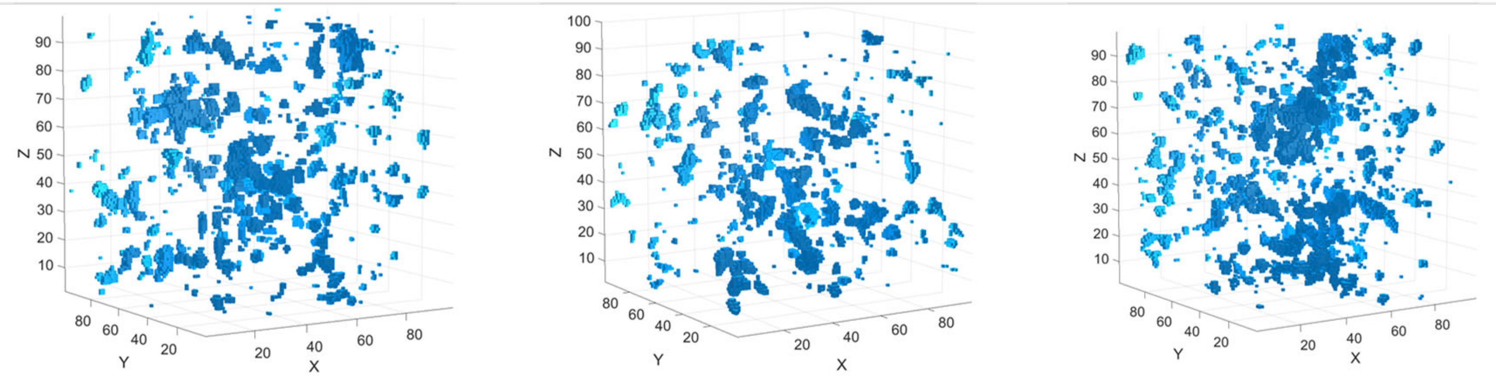

5.1% of total porosity = 0.93% of the REV	4.3% of total porosity = 0.73% of the REV	7.6% of total porosity = 1.35% of the REV

Closed pores visualization for the three REVs

Tortuosity

- Tortuosity is a measure of the deviation of the diffusion path through a porous medium from the straight-line, or Euclidean, distance; commonly defined as the **ratio of the actual path length to the straight-line distance between the start and end points**.
- It is needed to compute the effective diffusivity of species in a porous media.

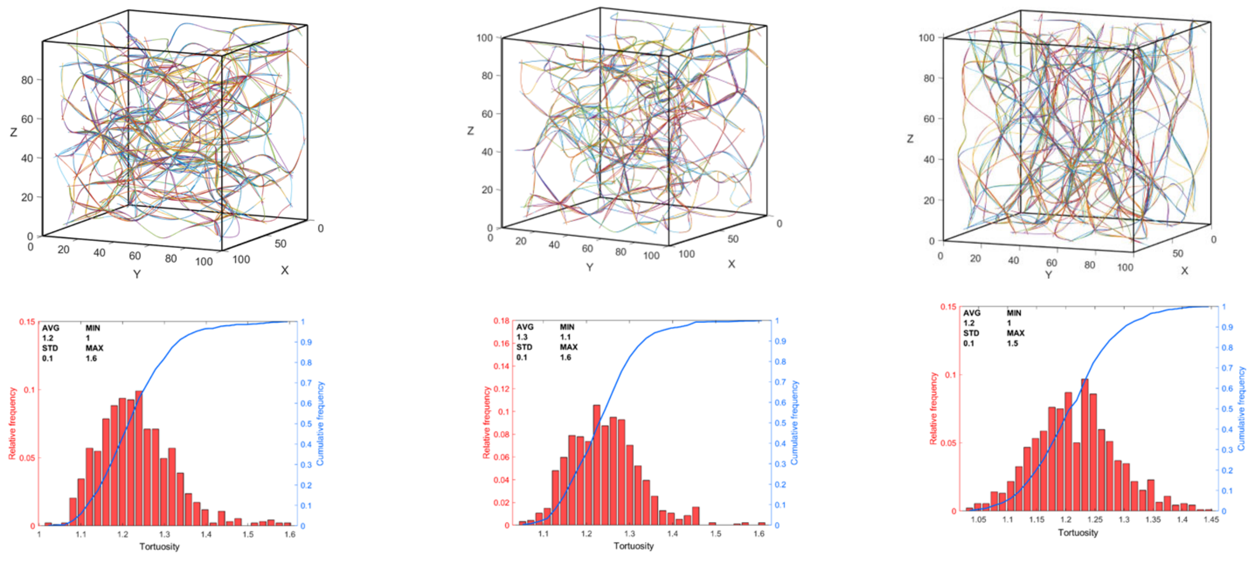

X Y Z

Average Tortuosity ~ 1.2

Ongoing Work

- Similar analysis will be carried out for other grades (ZXF-5Q, IG-110, NBG-18 and PCEA) for comparison of diffusive behaviors of different particles between grades.
- The pore morphology will be ported as realistic input for **phase field simulations**.

Thank You!

References

- Berre, C., et al. (2008). "Failure analysis of the effects of porosity in thermally oxidized nuclear graphite using finite element modelling." Journal of Nuclear Materials **381**(1-2): 1-8.
- Liu, F., et al., *The pores evolution in 3D view of nuclear graphite under ion beam irradiation.* Journal of Nuclear Materials, 2021. **557**: p. 153262.
- Sumita, J., et al. (2014). "Development of evaluation method with X-ray tomography for material property of IG-430 graphite for VHTR/HTGR." Nuclear Engineering and Design **271**: 314-317.
- Guo, J.-T., et al. (2022). "Measurement of pore diffusion factor of porous solid materials." Petroleum Science **19**(4): 1897-1904.